Geomechanics and Engineering, *Vol. 20, No. 5 (2020) 411-420*
DOI: https://doi.org/10.12989/gae.2020.20.5.411

A simplified directly determination of soil-water retention curve from pore size distribution

Geng Niu[1,2a], Longtan Shao[*1], De'an Sun[3b] and Xiaoxia Guo[1,2c]

[1]State Key Laboratory of Structural Analysis for Industrial Equipment, Dalian University of Technology, 116024 Dalian, Liaoning Province, China
[2]Department of Engineering Mechanics, Dalian University of Technology, 116024 Dalian, Liaoning Province, China
[3]Department of Civil Engineering, Shanghai University, 200444 Shanghai, China

(Received November 4, 2019, Revised February 5, 2020, Accepted February 6, 2020)

Abstract. Numbers fitting-curve equations have been proposed to predict soil-water retention curve (SWRC) whose parameters have no definitude physical meaning. And these methods with precondition of measuring SWRC data is time-consuming. A simplified directly method to estimate SWRC without parameters obtained by fitting-curve is proposed. Firstly, the total SWRC can be discretized into linear segments respectively. Every segment can be represented by linear formulation and every turning point can be determined by the pore-size distribution (PSD) of Mercury Intrusion Porosimetry (MIP) tests. The pore diameters governing the air-entry condition (AEC) and residual condition (RC) can be determined by the PSDs of MIP test. The PSD changes significantly during drying in SWR test, so the determination of AEC and RC should use the PSD under corresponding suction conditions. Every parameter in proposed equations can be determined directly by PSD without curve-fitting procedure and has definitude physical meaning. The proposed equations give a good estimation of both unimodal and bimodal SWRCs.

Keywords: soil water retention curve; pore size distribution; air-entry condition; residual condition; mercury intrusion porosimetry

1. Introduction

Soil-water retention curve (SWRC), which defines the relationship between water content and matric suction in soils contains the fundamental theory describing mechanical behaviors of unsaturated soil (Fredlund and Rahardjo 1993). SWRC can be employed to predict the permeability coefficient (Leong and Rahardjo 1997, Xu 2004), shear strength (Vanapalli *et al.* 1996, Zhou *et al.* 2016), deformation (Zhou *et al.* 2012, Gao *et al.* 2018), water migration (Oren *et al.* 2018, Zhu *et al.* 2018) and constitutive modelling of unsaturated soil (Sheng *et al.* 2004, Zhou *et al.* 2017). The success of the implementation of unsaturated soil mechanics into geotechnical engineering practice depends largely on water content and state of water in soils, especially the degree of saturation (An *et al.* 2018).

The SWRC is commonly determined by tests in laboratory. Axis-translation method (ATM)(0-1.5 MPa), filter paper method (FPM)(0.3-25 MPa) and vapor equilibrium technique with saturated salt solution (VET)(3-367 MPa) are generally employed to investigate the water retention behaviors of soils over a wide suction range (Gao and Sun 2017). The main hindrances to the direct determination of SWRC in the laboratory are time-consuming and overelaborate procedure (Chin *et al.* 2010). In order to overcome this limitation, numerous closed-form and empirical equations have been proposed to describe the SWRC (e.g., BC model (Brook and Corey 1964); VG model (Van Genuchten 1980); FX model (Fredlund and Xing 1994). Difficulties in the application of the previous equations exist because the parameters of these equations are not individually related to shape features of the SWRC. More development of SWRC estimations has been extended from a couple of the basic properties and parameters in SWRC equations are based on the statistical analysis from a great deal of experimental data (Chin *et al.* 2010).

Water retention behavior in soils is highly dependent on the individual pores, providing water-soil interactions mainly governed by capillarity (Xu 2004, Sun *et al.* 2016). So, many simple methods of determining SWRC indirectly are presented from pore size distribution (PSD) in Mercury Intrusion Porosimetry (MIP) test (Aung *et al.* 2001, Romero 1999, Zhang *et al.* 2018a). But most calculated curves from MIP test can't match test data quite well. The PSD changes significantly during the SWRC test which can cause the discrepancies between predicted and measured curves (Simms and Yanful 2002, Salager *et al.* 2013).

Unimodal and bimodal SWRCs can be discretized simply as three and five linear segments respectively.

*Corresponding author, Professor
E-mail: shaolt@dlut.edu.cn, shaolt@hotmail.com
[a]Ph.D.
E-mail: niugeng@mail.dlut.edu.cn
[b]Professor
E-mail: sundean@shu.edu.cn
[c]Professor
E-mail: hanyuer@dlut.edu.cn

http://www.techno-press.org/?journal=gae&subpage=7
ISSN: 2005-307X (Print), 2092-6219 (Online)

Another solution is to directly substitute the key parameters of SWRC into the equation such as the slopes and intersection points between linear segments of the curve (Pham and Fredlund 2008, Wijaya and Leong 2016). But, the measured SWRC data should be obtained firstly used to determine the parameters in these equations by fitting-curve.

To overcome these problems and limitations, a simplified determination of SWRC has been proposed based on discretizing the curve into linear segments respectively. Every segment can be represented by linear formulation and every turning point can be determined by the PSDs in MIP tests. The simplified SWRC equations have the advantage of mathematical simplicity and every parameter has definite physical meaning.

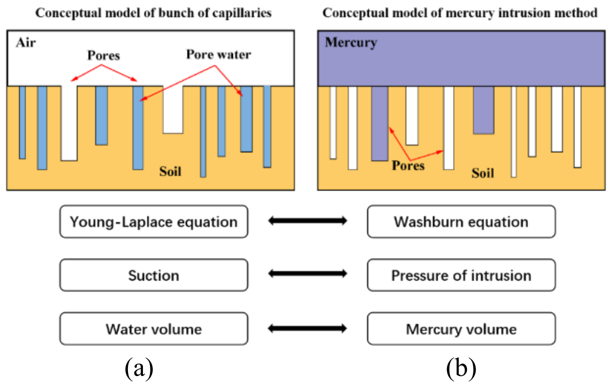

Fig. 1 Schematic of the models: (a) Conceptual sketch of a bundle of cylindrical capillaries and (b) Conceptual model of mercury intrusion method

2. Literature review

There are various best fitting-curve equations for SWRC proposed by different researchers (Fredlund 2019). At present, the equations have the following types: two-fitting parameter, three-fitting parameter and four-fitting parameter (Fredlund 2019). These empirical formulas can be used to estimate SWRC over a wide suction range based on limited measured data points, which can be substituted in various constitutive models accessibly. Gardner (1958) proposed early the relationship between water content and suction in order to describe the permeability of soil. In a later effort, Brooks and Corey (1964) divided the SWRC into two stages by the turning point of AEV and each section can be represented by an equation respectively (BC Equation). Van Genuchten (1980) modified BC equation to enable more an accurate description in the nearly saturated condition, especially for clays. Fredlund and Xing (1994) proposed an equation (FX Equation) basing on the assumption that the shape of SWRC is governed by PSD respectively. And it's more valid in the high suction range with correction factor $C(w)$. Although it's not necessarily valid for all soils, FX equation is widely accepted to describe water retention behavior of soils among these SWRC models (Leong and Rahardjo 1997). But it's difficult to obtain the four fitting parameters and limited by the inexplicit meanings of the parameters.

The main limitation in empirical SWRC is the difficulty to obtain the fitting parameters (Chin *et al.* 2010). To overcome this limitation, a number of methods without the experimental measurement and fitting-curve have been proposed previously for the direct estimation of SWRC. In the past few decades, many attempts have been made to directly estimate SWRC based on the direst soil properties (e.g., texture and grain-size distribution (GSD) (Chin *et al.* 2010; Russell 2014). The most approach involves a conversion of the relationship between GSD (or PSD) and plasticity index (I_p) and water contents (Chin *et al.* 2010). The relationship between properties of soils and SWRC is generally obtained by fitting a large number of experiments. So the lack of physical meaning for the formula is also undesirable. Estimation techniques are attractive, but the associated assumptions and limitation must be kept in mind. Some direct estimations of SWRC are based on physical modeling (Xu 2004). These models are based on some assumptions considered not suitable.

In general, SWRC can be divided into unimodal and bimodal SWRC according to the type of PSD. And most models only focus on unimodal SWRC which isn't valid for bimodal SWRC. Zhang and Chen (2005) extended the FX model (Fredlund and Xing 1994) and the VG model (Van Genuchten 1980) to describe bimodal and multimodal SWRCs. Li *et al.* (2014) predict bimodal SWRC and permeability functions using physically based parameters. The best-fit equations are normally governed by a few fitting parameters typically determined using a curve fitting technique. These models are most based on unimodal SWRC model by fitting-curve and have no has definitude physical meaning for fitting parameters.

The assumption that a suction results from the capillary force of a certain pore diameter in water retention curve can be applicable based on the bundle of cylindrical capillaries (BCC) model. MIP test has been used reliably to determine total pore volume and PSD of soils (Aung *et al.* 2001, Chen *et al.* 2019, Wu *et al.* 2019). The basic theory used in the MIP test is similar to the Young-Laplace equation used in the water retention behavior. So, a simple method of determining SWRC indirectly is presented from PSD in MIP test (Aung *et al.* 2001, Romero 1999, Zhang *et al.* 2018a). But most calculated curves from MIP test can't match test data quite well. The PSD changes significantly during the SWRC test, while the assumption that the PSD is constant during drying in the calculation is adopted (Simms and Yanful 2002). And this change can cause the discrepancies between predicted and measured curves (Salager *et al.* 2013). Simms and Yanful (2002) proposed a spreadsheet method to model the evaluation of the PSD during drying and to estimate SWRC.

3. The estimation of SWRC from MIP considering shrinkage

Matric suction is mainly shown in the form of capillary force in a certain range, which reflects the action of the capillary force to the soil water (Kong and Tan 2000). Early

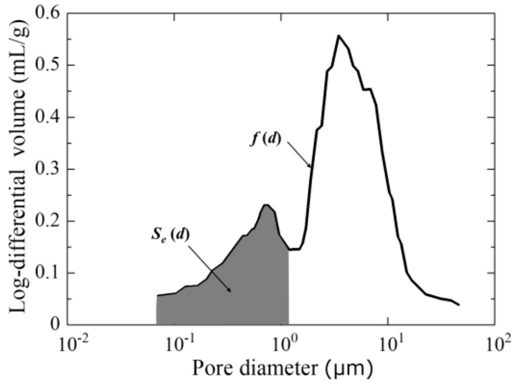

Fig. 2 The effective degree of saturation calculated by PSD of MIP test

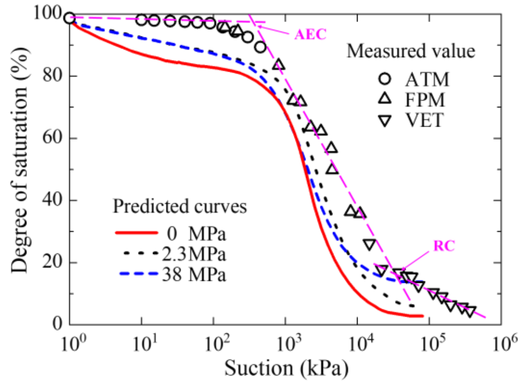

Fig. 4 SWRCs obtained by PSDs subjected to different maximum suctions

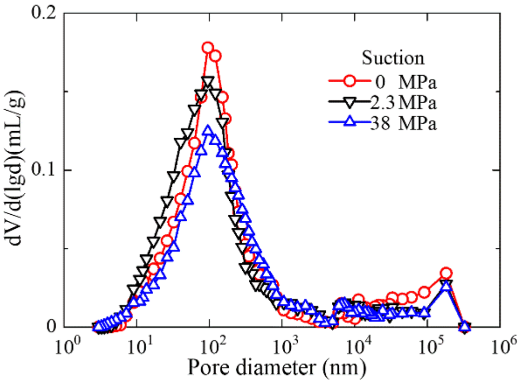

Fig. 3 PSDs of soils subjected to different maximum suctions (data from Niu *et al.* (2019))

conceptual models for the water distribution in pores of soils are based on BCC conceptualizing the pores in soils as an assembly of parallel capillary tubes to represent the pore geometry (Or and Tuller 2002). As illustrated in Fig. 1(a), there will be a definitive pore diameter according to the Young-Laplace equation, when given a certain suction. And basing on BCC model, the pores with a larger diameter than the certain one are completely empty, whereas smaller pores are completely filled with water (Romero 1999, Kong and Tan 2000, Lebeau and Konrad 2010). The relationship between suction and pore diameter can be derived from:

$$\psi_m = s = \frac{4T_{\mathrm{w}}cos\alpha_{\mathrm{w}}}{d} \tag{1}$$

where ψ_m is suction; s is general suction; Tw is the water-gas interfacial tension at 20°C (treated as 0.072 N/m); $cos\alpha_w$ is the water-soil contact angle (treated as 0); d is pore diameter.

MIP test has been used reliably to determine the pore volume and PSD in soils. As illustrated in Fig. 1(b), the principle of MIP is that the non-invasive liquid, mercury, will inflow into a solid void with the corresponding radius under the pressure during pressure increasing (Aung *et al.* 2001). Washburn's equation (Washburn 1921) derived for capillary flow of a liquid in a cylindrical tube is employed to calculate pore diameters based on the applied mercury pressures:

$$p(d) = \frac{4T_{\mathrm{m}}cos\alpha_{\mathrm{m}}}{d} \tag{2}$$

where p(d) is the pressure applied in MIP; T_m is the mercury surface tensions (treated as 0.485 N/m); $cos\alpha_m$ is the mercury-soil contact angle (treated as 130°); d is pore diameter.

Comparing Eqs. (1) and (2), there is a specific relationship between the pressure applied in MIP test and the suction in SWRC test:

$$\mathrm{s} = 0.196 * p(d) \tag{3}$$

As shown in Fig. 1(a), water retention behavior and cumulative intruded volume in MIP test are highly dependent on the individual pores and the basic theory used in the MIP test is similar to the capillary model. So cumulative intruded volume can be assimilated to air intrusion process in SWR tests. The intruded volume of mercury is equivalent to the water volume removed from the pores by the air intrusion for the same diameter of pores being intruded (Sun *et al.* 2016). There is a specific relationship between the pressure applied in MIP test and the suction in SWRC test (Sun *et al.* 2016, Zhang *et al.* 2018b), as summarized in Eq. (3). As illustrated in Fig. 2, the effective water content (such as the effective degree of saturation) can be calculated by mercury intruded volume:

$$S_e = \frac{\int_{d_{min}}^{d} f(d)\mathrm{d}d}{\int_{d_{min}}^{d_{max}} f(d)\mathrm{d}d} \tag{4}$$

where S_e is the effective degree of saturation; d is the pore diameter; d_{min} is the smallest pore diameter and d_{max} is the largest pore diameter in MIP test; $f(d)$ is the PSD as a function of pore diameter.

There is a difference between the measured void ratio and the one obtained by MIP test can be considered as residual volume:

$$S_d = \frac{(e_{\mathrm{m}} - G_s c(d_{\mathrm{min}}))}{e_{\mathrm{m}}} \tag{5}$$

where S_d is the difference between the two measurement test in degree of saturation ("residual degree of saturation"); e_m is the void ratio obtained directly; $c(d_{min})$ is the cumulative intruded volume finally; G_s is the specific gravity.

There is a relationship between the degree of saturation, effective degree of saturation and "residual degree of

Table 1 Physical property index of complete-intense weathering mudstone

Natural water content (%)	Natural dry density (g/cm^3)	Natural degree of saturated (%)	Specific gravity	Maximum dry density (g/cm^3)	Optimum water content (%)	Liquid limit (%)	Plastic limit (%)	Free swelling ratio (%)
28	1.48	98	2.70	1.78	17	52.6	25.9	29.9

saturation":

$$S_r = S_e(1 - S_d) + S_d \quad (6)$$

The research results show that PSD obtained by MIP can be used to predict the SWRC based on Young-Laplace equation and Washburn equation (Romero 1999, Aung *et al.* 2001, Sun *et al.* 2016, Zhang *et al.* 2018a). But most researchers obtain the SWRC by PSD can't match the experimental results reasonably well, especially in lower suction range. These methods are theoretically justified with the assumption that the volume of soil will not decrease as the water content is reduced or the suction is increasing. In this case, errors between the experimental values and predictions should not be neglected in soils, specifically in deformable clays.

In order to overcome the limitation of deformation in prediction of SWRC from MIP test, three PSDs of undisturbed complete-intense weathering mudstone undergoing different suctions (0, 2.3 and 38 MPa) respectively are shown in Fig. 3 (Niu *et al.* 2019). Table 1 summarizes the physical and mechanical property indexes of the clays. Although the types of the PSDs under different suctions are basically unimodal, the proportions in different pore diameters are different. Fig. 4 shows the calculated SWRC over a wide suction range determined by the three PSDs. There are obvious differences between the three predicted curves obtained by Eqs. (4), (5) and (6). And the discrepancies between predicted and measured curves are caused by the deformation during drying and the different flow paths in MIP and SWRC tests. The curve calculated by the PSD of soil with 0 kPa suction is less successful in predicting the water retention behavior in total suction range. The curve obtained by the PSD under 2.3 MPa suction can match the measured results better in middle suction range. And the curve obtained by the PSD under 38MPa suction is more successful in predicting the water retention behavior in higher suction range. These experimental results support the view shrinkage during drying can change PSD significantly.

4. The relationship between PSD and SWRC

Water retention in soils is highly dependent on the individual pores and the concept of PSD is more commonly used to explain the soil water retention behavior (Fredlund and Xing 1994, Sun *et al.* 2016). The assumption that a suction results from the capillary force of a certain pore diameter in the soil-water system for an unsaturated soil can be applied basing on BCC model. The researches of micro-scale tests (e.g., MIP, scanning electron microscope (SEM) and nuclear magnetic resonance (NMR)) show that the pore structure of soil samples can be divided into unimodal, bimodal and even multimodal PSD. The SWRC of samples

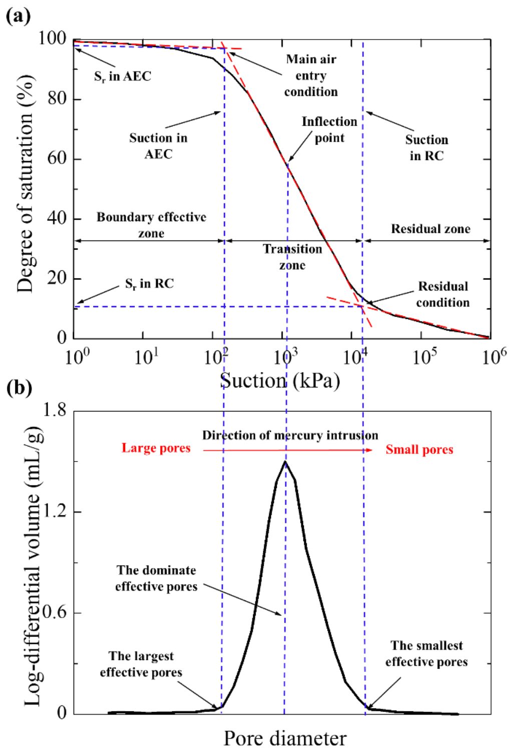

Fig. 5 The relationship between typical unimodal SWRC and PSD: (a) Typical unimodal SWRC and (b) Unimodal PSD

with unimodal PSD has a typical shape of "S", while the one with bimodal PSD has a "horizontal stage" in transition zone based on BCC model (Sun *et al.* 2016).

Fig. 5(a) shows the typical SWRC in the total suction range and there are two distinct changes in slope from the curve. The changes in slope define two points that are pivotal to describing the SWRC. The first point is termed the air-entry condition (AEC) of the soil, where the air starts to enter the soil pores obviously as suction increasing. The second point is termed residual condition (RC), where it becomes significantly more difficult to remove water as suction increasing in a larger value. (Fredlund *et al.* 2011). According to BCC model and Young-Laplace equation, AEV is the suction, where the largest effective pores start draining (Brooks and Corey 1964, Fredlund and Xing 1994) and RC involves the suction and water content, where the smallest effective pores start draining. The dependency of SWRC on PSD depicted in Fig. 5(b) shows that the pores governing the AEC where mercury intrude obviously are the largest effective pores and the pores governing the RC where it becomes significantly more difficult to intrude mercury as pressure increasing. The inflection point in SWRC corresponds to the dominant pore diameter where the peak of PSD curve.

When two or more pore families exist in soils, the

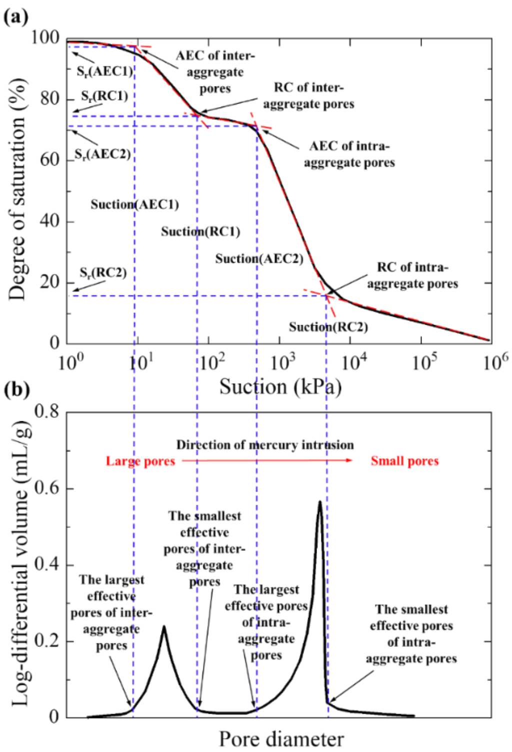

Fig. 6 The relationship between typical unimodal SWRC and PSD: (a) Typical unimodal SWRC and (b) Unimodal PSD

Table 2 Statistics on air entry values for different soils

No.	Soils	Suction in AEC (kPa)	S_r in AEC (%)	Reference
1	Regina clay	2200	97	Fredlund and Xing (1994)
2	Indian Head till	80	98	Vanapalli *et al.* (1996)
3	Weakly expansive soil	40	97	Zhang *et al.* (2015)
4	Silty loam	50	98	Brook and Corey (1964)
5	Granitic residual soil	270	98	Aung *et al.* (2001)
6	Complete-intense weathering mudstone	327	97	Niu *et al.*, (2019)
7	Sarnia clay	220	97	Simms and Yanful (2002)
8	Touchet silt loam	6	98	Leong and Rahardjo (1997)
9	Compacted fine sand with kaolin	30	98	Zhai and Rahardjo (2012)
10	Pearl clay	75	97	Gao and Sun (2017)
11	Lateritic clay	18	98	Sun *et al.* (2016)
12	Boom clay	413	97	Romero (1999)
13	A clayey silty sand	38	98	Salager *et al.* (2013)

corresponding SWRC can be bimodal or multimodal. As shown in Fig. 6(a), there are two lines with different slopes in the typical transition zone forming two AECs and RCs respectively. The largest effective pores governing the AEC and the smallest effective pores governing the RC following the aforementioned rules. The first AEC is governed by the largest effective pores of peak 1 in inter-aggregate pores and the second AEC is governed by the largest effective pores of peak 2 in intra-aggregate pores, as illustrated in Fig. 6(b). Similarly, the first RC is governed by the smallest effective pores of peak 1 in inter-aggregate pores and the second RC is governed by the smallest effective pores of peak 2 in intra-aggregate pores. And the two inflection points in every transition zone also correspond to the pore diameter in the peaks of the PSD curve.

For soils with larger expansibility and shrinkage, the pores governing the RC where it becomes significantly more difficult to intrude mercury as pressure increasing should be determined by the PSD of soils undergoing higher suction. Because the PSD is different in different suction condition, and calculated suction and water retention obtained from different saturated conditions in RC are different, as illustrated in Figs. 3 and 4. As shown in Fig. 4, the AEV of the undisturbed soils is about 350 kPa and the suction of RC is about 4×10^4 kPa (residual degree of saturation is about 15%). From Fig. 3, the pore diameter of the undisturbed samples which control AEV is about 747 nm, and the pore diameter which controls the residual degree of saturation is about 7 nm. According to Eq. (3), the suctions at AEV and RC are about 327 kPa and 3.8×10^4 kPa and the calculated

residual degree of saturation is about 15% based on Eq. (6). This further proves the correctness of the mentioned relationship between PSD and SWRC.

Some parameters in SWRC such as AEV, the slope at the inflection point, water content and suction at RC are commonly used to describe the SWRC and other associated properties. These parameters are generally determined from the graphical method which is subjective. In the conventional graphical method, errors associated with the manual drawing of the tangent line on the curve at a certain point can result in variability in the determination of AEC and RC (Zhai and Rahardjo 2012). The pore diameters with definite physical meaning governing the AEC and RC can be determined by the PSD of MIP test, which can be replaced the conventional graphical method in providing consistent results.

5. A simplified method to estimate SWRC

As the typical SWRC shape shown in Fig. 5(a), there are two key points in the curve generally, where the three distinct changes in slope. The unimodal SWRC can be discretized into three zones, namely (I) nearly saturated portion from saturated condition to AEC, (II) an intermediate portion from AEC to RC, and (Ш) residual portion from RC to "zero water storage" point (suction is 106 kPa) (Pham and Fedlund 2008). The three equations of three zones cover the entire suction range can be written as follows:

$$\begin{aligned} w_{\mathrm{I}} &= w_{\mathrm{s}} - s_{\mathrm{I}}\log(\psi) && \psi \le \psi_{AEC} \\ w_{\mathrm{II}} &= w_{\mathrm{aev}} - s_{\mathrm{II}}\log\left(\frac{\psi}{\psi_{\mathrm{aev}}}\right) && \psi_{AEC} \le \psi \le \psi_{RC} \\ w_{\mathrm{III}} &= s_{\mathrm{III}}\log\left(\frac{10^6}{\psi}\right) && \psi \ge \psi_{RC} \end{aligned} \quad (7)$$

where w_{I},w_{II},w_{III} are water contents in three portions; s_{I}, s_{II} and s_{III} are the slopes of the straight lines in three portions; ψ is suction.

Although the method is simple, the water contents at the start and end points of each line segment and the three slopes are difficult to determine. Moreover, it is difficult to determine the suctions in AEC and RC. Basing on the recent findings by Pham and Fredlund (2008), the SWRC can be predicted directly, if the water contents and suctions only in AEC and RC are determined. From the last section, the pores where mercury intrudes obviously is the largest effective pores, which govern the AEC, and the smallest effective pores governing the RC, where it becomes significantly more difficult to intrude mercury as pressure increasing, as shown in Figs. 5 and 6. If the largest and smallest effective pore diameters can be determined, then the suction and degree of saturation in AEC and RC can be obtained respectively by the Eqs. (3), (4), (5) and (6).

It can be seen in Fig. 4, although the predicted curve couldn't match the measured results quilt well, the suction of AEC calculated by the largest pore diameter determined by MIP is closely approximate to AEV obtained by SWRC test. But, the water content in AEC calculated by PSD is different from the one defined by SWRC test. In order to investigate the degree of saturation in AEC, a total of 13 independent suctions of AEC with silts and clays are tabulated respectively in Table 2. Through the review, the assumption that the degree of saturation in AEC of most silts is about 98% and 97% for most clays can be established.

Inspection of Fig. 4 shows that the suction and degree of saturation in RC can be obtained reasonably by the PSD of soil with 38 MPa suction according to Eqs. (3), (4), (5) and (6). It is also usually assumed that it is reasonable to determine the suction and water content in RC by the PSD under saturated condition (suction is 0 kPa) for silts and clays without significant deformation during suction increasing.

If the suctions and degree of saturations in AEC and RC are determined, there are four intersection points for unimodal SWRC adding the saturated condition (suction is about 0.1 kPa and degree of saturation is 100%) and "zero water storage" condition (suction is about 10^6 kPa and degree of saturation is 0). SWRC in total suction range can be discretized as three linear segments, respectively (Pham and Fedlund 2008, Wijaya and Leong 2016). The SWRC equations discretized as three linear segments can be described as follows

$$
\begin{aligned}
S_r &= -\frac{1-S_{r_{\mathrm{AEC}}}}{\log\left(\frac{\psi_{\mathrm{AEC}}}{0.1}\right)}\log\psi + 1 && \psi \le \psi_{\mathrm{AEC}}\ \psi \le \psi_{\mathrm{AEC}} \\
S_r &= -\frac{S_{r_{\mathrm{AEC}}}-S_{r_{\mathrm{RC}}}}{\log\left(\frac{\psi_{\mathrm{RC}}}{\psi_{\mathrm{AEC}}}\right)}\log\psi + S_{r_{\mathrm{AEC}}} + \frac{S_{r_{\mathrm{AEC}}}-S_{r_{\mathrm{RC}}}}{\log\left(\frac{\psi_{\mathrm{RC}}}{\psi_{\mathrm{AEC}}}\right)}\quad \psi_{\mathrm{AEC}} && \psi_{\mathrm{AEC}} \le \psi \le \psi_{\mathrm{RC}} \\
S_r &= -\frac{S_{r_{RC}}}{\log\left(\frac{10^6}{\psi_{RC}}\right)}\log\psi + S_{r_{RC}} + \frac{S_{r_{RC}}}{\log\left(\frac{10^6}{\psi_{RC}}\right)}\quad \psi_{RC} && \psi \ge \psi_{\mathrm{RC}}
\end{aligned}
\tag{8}
$$

where S_{r} is degree of saturation; Ψ is suction; $S_{r\mathrm{AEC}}$ and $S_{r\mathrm{RC}}$ are the degree of saturations in AEC and RC respectively; Ψ_{AEC} and Ψ_{RC} are the matric suctions in AEC and RC respectively.

For the bimodal SWRC, there are two AECs and RCs respectively. The total SWRC can be also discretized into linear segments respectively. So there are 4 line segments and 6 turning points between every two line segments. Every segment can be represented by linear formulation. The equations for bimodal SWRC have a similar form with the ones of unimodal SWRC:

$$
\begin{aligned}
S_{\mathrm{r}} &= 1 - \frac{1-S_{\mathrm{r_{AEC1}}}}{\log\left(\frac{\psi_{\mathrm{AEC1}}}{0.1}\right)}\log\psi && \psi \le \psi_{\mathrm{AEC1}} \\
S_{\mathrm{r}} &= \frac{S_{\mathrm{r_{RC1}}}-S_{\mathrm{r_{AEC1}}}}{\log\left(\frac{\psi_{\mathrm{RC1}}}{\psi_{\mathrm{AEC1}}}\right)}\log\psi + S_{\mathrm{r_{AEC1}}} - \frac{S_{\mathrm{r_{RC1}}}-S_{\mathrm{r_{AEC1}}}}{\log\left(\frac{\psi_{\mathrm{RC1}}}{\psi_{\mathrm{AEC1}}}\right)}\psi_{\mathrm{AEC1}} && \psi_{\mathrm{AEC1}} \le \psi \le \psi_{\mathrm{RC1}} \\
S_{\mathrm{r}} &= \frac{S_{\mathrm{r_{AEC2}}}-S_{\mathrm{r_{RC1}}}}{\log\left(\frac{\psi_{\mathrm{AEC2}}}{\psi_{\mathrm{RC1}}}\right)}\log\psi + S_{\mathrm{r_{RC1}}} - \frac{S_{\mathrm{r_{AEC2}}}-S_{\mathrm{r_{RC1}}}}{\log\left(\frac{\psi_{\mathrm{AEC2}}}{\psi_{\mathrm{RC1}}}\right)}\psi_{\mathrm{RC1}} && \psi_{\mathrm{RC1}} \le \psi \le \psi_{\mathrm{AEC2}} \\
S_{\mathrm{r}} &= \frac{S_{\mathrm{r_{RC2}}}-S_{\mathrm{r_{AEC2}}}}{\log\left(\frac{\psi_{\mathrm{RC2}}}{\psi_{\mathrm{AEC2}}}\right)}\log\psi + S_{\mathrm{r_{AEC2}}} - \frac{S_{\mathrm{r_{RC2}}}-S_{\mathrm{r_{AEC2}}}}{\log\left(\frac{\psi_{\mathrm{RC2}}}{\psi_{\mathrm{AEC2}}}\right)}\psi_{\mathrm{AEC2}} && \psi_{\mathrm{AEC2}} \le \psi \le \psi_{\mathrm{RC2}} \\
S_{\mathrm{r}} &= -\frac{S_{\mathrm{r_{RC2}}}}{\log\left(\frac{10^6}{\psi_{\mathrm{RC2}}}\right)}\log\psi + S_{\mathrm{r_{RC2}}} + \frac{S_{\mathrm{r_{RC}}}}{\log\left(\frac{10^6}{\psi_{\mathrm{RC2}}}\right)}\psi_{\mathrm{RC2}} && \psi \ge \psi_{\mathrm{RC2}}
\end{aligned}
\tag{9}
$$

where S_{r} is degree of saturation; Ψ is matric suction; S_{r}AEC1 and S_{r}RC1 are the degree of saturations for inter-aggregate pores in AEC and RC respectively; S_{r}AEC2 and S_{r}RC2 are the degree of saturations for intra-aggregate pores in AEC and RC respectively; Ψ_{AEC1} and Ψ_{RC1} are the matric suctions for inter-aggregate pores in AEC and RC respectively; Ψ_{AEC2} and Ψ_{RC2} are the matric suctions for intra-aggregate pores in AEC and RC respectively.

There are four parameters in equations for unimodal SWRC and six parameters for bimodal SWRC which can be determined by the PSDs from MIP tests. And. It's not necessary to get SWRC data firstly. Moreover, this method to structure SWRC without fitting the experimental data and the parameters in proposed equations have explicit physical meanings respectively.

6. Evaluation of the proposed method

The validity of the proposed method is demonstrated by comparing predictions with experimental data on three different soils. The procedure is tested on SWRC and MIP tests obtained on three materials: undisturbed complete-intense weathering mudstone (w_{L}= 52.6%, I_{p}= 26.7) (Niu *et al.* 2019); Pearl clay (a silt, w_{L}= 43%, I_{p}= 26%) (Gao and Sun 2017) and lateritic clay (w_{L}= 78%, I_{p}= 36) (Sun *et al.* 2016).

6.1 Complete-intense weathering mudstone (clay)

Complete-intense weathering mudstone is taken from a landslip in The Guangxi Zhuang Autonomous Region, China. As have high liquid limit and plastic limit, the clay is classified as high liquid limit clay. Moreover, the free swelling ratio of this clay is about 29.9%. So shrinkage or swelling should be considered in the description of hydro-mechanics behaviors during drying and wetting progress.

Fig. 7 shows the PSDs of complete-intense weathering mudstone with different suctions (0 and 38 MPa). As illustrated in Fig. 7, the effective largest pore diameter governing AEC can be determined by the PSD under 0 kPa suction condition, and the suction (AEV) in AEC can be obtained by Eqs. (1)-(3). Complete-intense weathering mudstone is referred to as a clay according to the physical

Table 3 The parameters obtained by PSDs for complete-intense weathering mudstone

PSD at 0 MPa	d_{max} (nm)	747
	Pressure (psi)	241
	Suction at AEC (kPa)	327
	S_r at AEC (%)	97
PSD at 38 MPa	d_{min} (nm)	7
	Pressure (psi)	28080
	Suction at RC (kPa)	37930
	Calculated S_r at RC (%)	15

Table 4 The parameters obtained by PSD for Pearl clay

PSD at 0 MPa	d_{max} (nm)	1057
	Pressure (psi)	171
	Suction at AEC (kPa)	231
	S_r at AEC (%)	98
	d_{min} (nm)	151
	Pressure (psi)	1196
	Suction at RC (kPa)	1615
	Calculated S_r at RC (%)	6

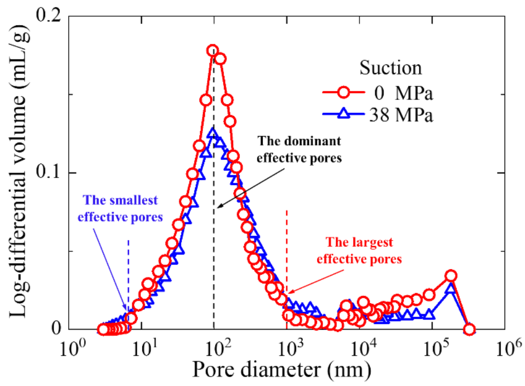

Fig. 7 PSDs of soils subjected to different suctions

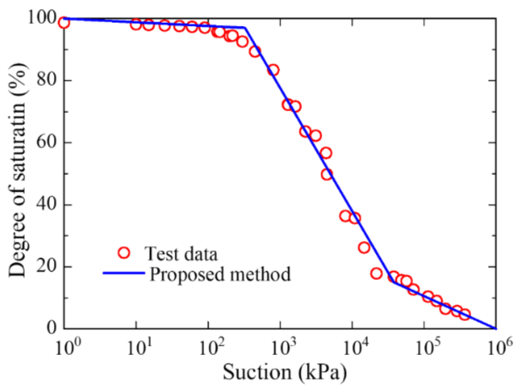

Fig. 8 Comparison of predicted and measured SWRCs for complete-intense weathering mudstone

properties, so the degree of saturated in AEC is about 97%. The smallest effective pore diameter governing RC can be determined by the PSD under 38 MPa suction condition, then the suction and degree of saturation in RC can be obtained by Eqs. (1)-(3) and Eqs. (4)-(6) respectively. The parameters in SWRC equations obtained by PSDs for complete-intense weathering mudstone are illustrated in Table 3. Substitution of the parameters into Eq. (8) leads to the SWRC of undisturbed complete-intense weathering mudstone. As illustrated in Fig. 8, the predicted SWRC obtained by the proposed method can match the experimental data well.

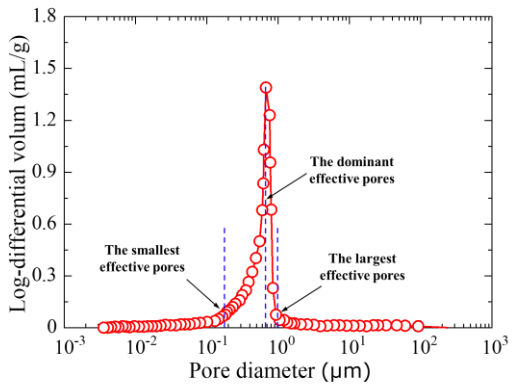

Fig. 9 PSDs of Pearl clay subjected to different maximum suctions (data from Gao and Sun 2017)

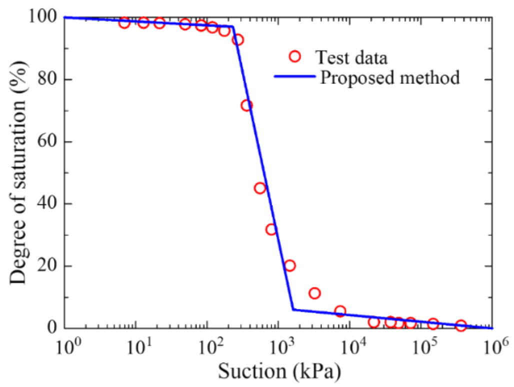

Fig. 10 PSDs of Pearl clay subjected to different maximum suctions (data from Gao and Sun 2017)

6.2 Pearl clay (silt)

The clay mineralogy compositions for Pearl clay, determined using the X-ray diffraction test, include quartz, pyrophyllite, and kaolinite in the dominant order (Gao and Sun 2017). There is little expansive clay mineral in Pearl clay. So the deformation can be neglected during drying and wetting progress. Moreover, the PSD at saturated condition can describe the PSD in every condition during drying.

Fig. 9 shows the PSD of reconstituted Pearl clay in the saturated condition, and it's a unimodal PSD. According to the procedure described in the last section, the largest effective pore diameter and smallest pore diameter can be determined by the PSD. Then the suctions in AEC and RC can be obtained by Eqs. (1)-(3) and the degree of saturation at RC can be obtained by Eqs. (4)-(6). As Pearl clay is referred to as a silt according to the physical properties and mineralogy compositions, the degree of saturation in AEC is about 98%. Table 4 summarizes the parameters in SWRC obtained by PSD for reconstituted Pearl clay. SWRC can be

Table 5 The parameters obtained by PSDs for Lateritic clay

PSD at 0 MPa	Peak 1	d_{max} of Peak 1 (nm)	12508
		Pressure at d_{max} of Peak 1 (psi)	14.46
		Suction from d_{max} of Peak 1 (kPa)	19.5
		d_{min} of Peak 1 (nm)	2110
		Pressure at d_{min} of Peak 1 (psi)	85.6
		Suction from d_{min} of Peak 1 (kPa)	116
		Calculated S_r in d_{min} of Peak 1 (%)	81
PSD at 38 MPa	Peak 2	d_{max} of Peak 2 (nm)	95.4
		Pressure at d_{max} of Peak 2 (psi)	1895
		Suction from d_{max} of Peak 2 (kPa)	2600
		Calculated S_r in d_{min} of Peak 2 (%)	74
		d_{min} of Peak 2 (nm)	7.2
		Pressure at d_{min} of Peak 2 (psi)	24985
		Suction from d_{min} of Peak 2 (kPa)	33700
		Calculated S_r in d_{min} of Peak 2 (%)	12

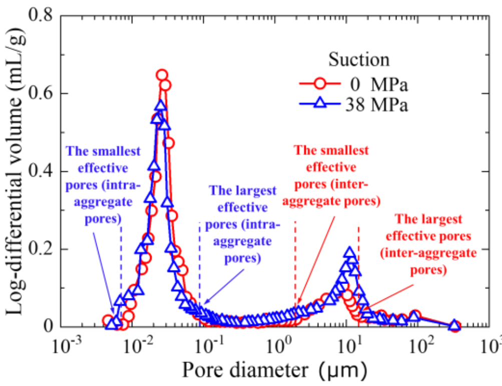

Fig. 11 PSDs of Lateritic clay subjected to different maximum suctions (data from Sun *et al.* 2016)

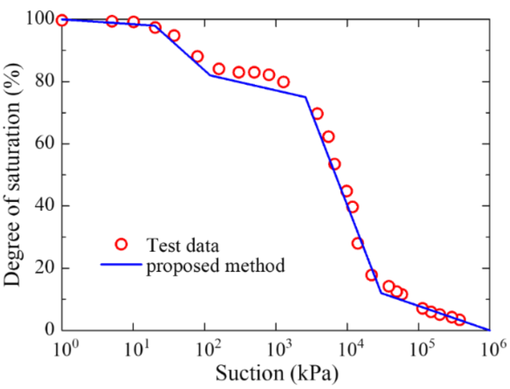

Fig. 12 Comparison of predicted and measured SWRCs for Lateritic clay

obtained by substituting the parameters determined from PSD into Eq. (8). Fig. 10 shows the measured and predicted results of the SWRC for reconstituted Pearl clay in the main drying (e=1.10). It can be seen that the prediction obtained by proposed equations is in good agreement with experimental data.

6.3 Lateritic clay (Bimodal SWRC)

The lateritic clay is taken at ground surface from Guilin in south China. The main mineral compositions of the soil are kaolinite, illite, goethite, and quartz determined usingX-ray diffraction (XRD) (Sun *et al.* 2016). Meanwhile, free iron oxides exist in lateritic clay, which strengthens the connection and the coating effect between particles. So lateritic clay generally exhibits a bimodal PSD and bimodal SWRC.

Fig. 11 shows the PSDs of compacted lateritic clay subjected to different suctions (0 and 38 MPa). As illustrated in Fig. 11, the samples with different saturation condition always exhibit distinct bimodal PSD. The largest effective pore diameter of peak 1 can be determined by the PSD under 0 kPa suction condition and the corresponding suction in AEC can be calculated by Eqs. (1)-(3). The degree of saturation is referred to as 98% because the lateritic soil is a clay. The smallest effective pore diameter of peak 1 can be determined by the PSD under 0 MPa suction condition, then the suction and degree of saturation in RC can be obtained by Eqs. (1)-(3) and Eqs. (4)-(6) respectively. Similarly, the largest effective pore diameter and smallest diameter of peak 2 can be determined by the PSD under 38 MPa suction condition. The suctions and degree of saturations in AEC and RC of peak 2 can be calculated by Eqs. (1)-(3) and Eqs. (4)-(6) respectively. The parameters obtained by PSDs are summarized in Table 5. Substitution of the parameters into Eq. (10) leads to the predicted SWRC of compacted lateritic clay as illustrated in Fig. 12. And it can be seen that the predicted curve can match test data quite well. So the proposed method can perform well for bimodal SWRC.

7. Conclusions

For typical unimodal SWRC, the largest effective pores govern the AEC, and the smallest effective pores govern the RC. Moreover, the inflection point in SWRC corresponds to the dominant pore diameter where the peak of PSD curve. For bimodal SWRC, the first AEC and RC are governed by the largest effective pores and smallest pores of peak 1 (inter-aggregate pores) of PSD respectively and the second AEC and RC are governed by the largest effective pores and smallest pores of peak 2 (intra-aggregate pores) of PSD respectively. The largest and smallest effective pore diameters can be determined by the PSDs of MIP tests in according conditions. The PSD changes significantly during drying in SWR test for deformable soils. A given PSD is representative of the unique SWRC, so the SWRCs obtained by PSDs of soils subjected to different suctions are different. The determination of AEC should use the PSD under lower suction condition, while defining RC by the PSD under higher suction condition.

Unimodal and bimodal SWRCs can be discretized as three and five linear segments respectively, and every segment can be represented by linear formulation. The simplified SWRC equations have been proposed, in which the bundle of the capillary model is employed. There are three parameters for unimodal SWRC and seven parameters for bimodal SWRC, which can be determined by PSDs of MIP tests. Every parameter in proposed equations has definitude physical meaning in proposed SWRC equations.

The proposed method is verified by experimental SWRC data of silts, deformable clays and clays with bimodal PSD. The advantages of proposed SWRC equations are (a) the experimental data of SWRC is not necessary, which can overcome the limitation of time-consuming in tests; (b) proposed equations can be performed well for unimodal and bimodal SWRCs; (c) every parameter in proposed equations can be determined directly by PSD without curve-fitting procedure and has definitude physical meaning; (d) proposed equations are performed considering deformation during drying progress.

Acknowledgments

This study was financially supported by National Key Laboratory Funding of Independent Research Project [grant number S18406]; National Natural Science Foundation of China [grant number 51479023, grant number 51909241], and National Natural Science Foundation of Liaoning [grant number 2019-ZD-0187].

References

An, N., Hemmati, S., Cui, Y.J. and Tang, C.S. (2018), "Numerical investigation of water evaporation from Fontainebleau sand in an environmental chamber", *Eng. Geol.*, **234**, 55-64. https://doi.org/10.1016/j.enggeo.2018.01.005.

Aung, K.K., Rahardjo, H., Leong, E.C. and Toll, D.G. (2001), "Relationship between porosimetry measurement and soil-water characteristic curve for an unsaturated residual soil", *Proceedings of the Unsaturated Soil Concepts and Their Application in Geotechnical Practice*, Dordrecht, The Netherlands.

Brooks, R.H. and Corey, A.T. (1964), "Hydraulic properties of porous media", Hydrology Paper No. 3, Civil Engineering Department, Colorado State University, Fort Collins, Colorado, U.S.A.

Chen, B., Sun, D.A. and Jin, P. (2019), "Experimental study of the effect of microstructure on the permeability of saturated soft clays", *Geomech. Eng.*, **18**(1), 49-58. https://doi.org/10.12989/gae.2019.18.1.049.

Chin, K.B., Leong, E.C. and Rahardjo, H. (2010), "A simplified method to estimate the soil-water characteristic curve", *Can. Geotech. J.*, **47**(12), 1382-1400. https://doi.org/10.1139/T10-033.

Fredlund, D.G. and Rahardjo, H. (1993), *Soil Mechanics for Unsaturated Soils*, Wiley, New York, U.S.A.

Fredlund, D.G. and Xing, A. (1994), "Equations for the soil-water characteristic curve", *Can. Geotech. J.*, **31**(4), 521-532. https://doi.org/10.1139/t94-061.

Fredlund, D.G., Sheng, D. and Zhao, J. (2011), "Estimation of soil suction from the soil-water characteristic curve", *Can. Geotech. J.*, **48**(2), 186-198. https://doi.org/10.1139/T10-060.

Fredlund, D.G. (2019), "State of practice for use of the soil-water characteristic curve in geotechnical engineering", *Can. Geotech. J.*, **56**, 1059-1069. https://doi.org/10.1139/cgj-2018-0434.

Gardner, W.R. (1958), "Some stead-state solution of the unsaturated moisture flow equation with application to evaporation from a water-table", *Soil Sci.*, **85**(4), 228-232. https://doi.org/10.1097/00010694-195804000-00006.

Gao, Y. and Sun, D.A. (2017), "Soil-water retention behavior of compacted soil with different densities over a wide suction range and its prediction", *Comput. Geotech.*, **91**, 17-26. https://doi.org/10.1016/j.compgeo.2017.06.016.

Gao, Y., Sun, D.A. and Wu, Y. (2018), "Volume change behaviour of unsaturated compacted weakly expansive soils", *Bull. Eng. Geol. Environ.*, **77**(2), 837-848. https://doi.org/10.1007/s10064-017-1142-0.

Gao, Y., Sun, D.A., Zhu, Z. and Xu, Y. (2019), "Hydromechanical behavior of unsaturated soil with different initial densities over a wide suction range", *Acta. Geotech.*, **14**(2), 417-428. https://doi.org/10.1007/s11440-018-0662-5.

Kong, L.W. and Tan, L.R. (2000), "A simple method of determining the soil-water characteristic curve indirectly", *Proceedings of the Asian Conference on Unsaturated Soils*, Singapore, May.

Lebeau, M. and Konrad, J.M. (2010), "A new capillary and thin film flow model for predicting the hydraulic conductivity of unsaturated porous media", *Water Resour. Res.*, **46**(12). https://doi.org/10.1029/2010WR009092.

Leong, E.C. and Rahardjo, H. (1997), "Review of soil-water characteristic curve equations", *J. Geotech. Geoenviron. Eng.*, **123**(12), 1106-1117. https://doi.org/10.1061/(ASCE)10900241(1997)123:12(1106).

Li, X., Li, J.H. and Zhang, L.M. (2014), "Predicting bimodal soil–water characteristic curves and permeability functions using physically based parameters", *Comput. Geotech.*, **57**, 85-96. https://doi.org/10.1016/j.compgeo.2014.01.004.

Niu, G., Sun, D.A., Shao, L. and Zeng, L. (2019), "The water retention behaviours and pore size distributions of undisturbed and remoulded complete-intense weathering mudstone", *Eur. J. Environ. Civ. Eng.*, 1-18. https://doi.org/10.1080/19648189.2019.1572544.

Or, D. and Tuller, M. (2002), "Cavitation during desaturation of porous media under tension", *Water Resour. Res.*, **38**(5), 19-1-19-14. https://doi.org/10.1029/2001WR000282.

Oren, A.H., Aksoy, Y.Y., Onal, O. and Demirkiran, H. (2018), "Correlating the hydraulic conductivities of GCLs with some properties of bentonites", *Geomech. Eng.*, **15**(5), 1091-1100. https://doi.org/10.12989/gae.2018.15.5.1091.

Pham, H.Q. and Fredlund, D.G. (2008), "Equations for the entire soil-water characteristic curve of a volume change soil", *Can. Geotech. J.*, **45**(4), 443-453. https://doi.org/10.1139/T07-117.

Romero, E. (1999), "Characterisation and thermo-hydro-mechanical behaviour of unsaturated Boom clay: An experimental study", Ph.D. Dissertation, Universitat Politècnica de Catalunya, Barcelona, Spain.

Russell, A.R. (2014), "How water retention in fractal soils depends on particle and pore sizes, shapes, volumes and surface areas", *Géotechnique*, **64**(5), 379-390. https://doi.org/10.1680/geot.13.P.165.

Salager, S., Nuth, M., Ferrari, A. and Laloui, L. (2013), "Investigation into water retention behaviour of deformable soils" *Can. Geotech. J.*, **50**(2), 200-208. https://doi.org/10.1139/cgj-2011-0409.

Sheng, D.C., Sloan, S.W. and Gens, A. (2004), "A constitutive model for unsaturated soils: thermomechanical and computational aspects", *Comput. Mech.*, **33**(6), 453-465. https://doi.org/10.1007/s00466-003-0545-x.

Simms, P.H. and Yanful, E.K. (2002), "Predicting soil-water characteristic curves of compacted plastic soils from measured pore-size distributions", *Géotechnique*, **52**(4), 269-278.

https://doi.org/10.1680/geot.2002.52.4.269.

Sun, D.A., Gao, Y., Zhou, A.N. and Sheng, D.C. (2016), "Soil-water retention curves and microstructures of undisturbed and compacted Guilin lateritic clay", *Bull. Eng. Geol. Environ.*, **75**(2), 781-791. https://doi.org/10.1007/s10064-015-0765-2.

Vanapalli, S.K., Fredlund, D.G., Pufahl, D.E. and Clifton, A.W. (1996), "Model for the prediction of shear strength with respect to soil suction", *Can. Geotech. J.*, **33**(3), 379-392. https://doi.org/10.1139/t96-060.

Van Genuchten, M.T. (1980), "A closed-form equation for predicting the hydraulic conductivity of unsaturated soils 1", *Soil Sci. Soc. Am. J.*, **44**(5), 892-898. https://doi.org/10.2136/sssaj1980.03615995004400050002x.

Washburn, E.W. (1921), "The dynamics of capillary flow", *Phys. Rev.*, **17**(3), 273. https://doi.org/10.1103/PhysRev.18.206.

Wijaya, M. and Leong, E.C. (2016), "Equation for unimodal and bimodal soil-water characteristic curves", *Soils Found.*, **56**(2), 291-300. https://doi.org/10.1016/j.sandf.2016.02.011.

Wu, Y., Jiang, H., Lu, Y. and Sun, D. (2019), "Experimental study on treatment of waste slurry by vacuum preloading with different conditioning agents", *Geomech. Eng.*, **17**(6), 543-551. https://doi.org/10.12989/gae.2019.17.6.543.

Xu, Y. (2004), "Calculation of unsaturated hydraulic conductivity using a fractal model for the pore-size distribution", *Comput. Geotech.*, **31**(7), 549-557. https://doi.org/10.1016/j.compgeo.2004.07.003.

Zhai, Q. and Rahardjo, H. (2012), "Determination of soil-water characteristic curve variables", *Comput. Geotech.*, **42**, 37-43. https://doi.org/10.1016/j.compgeo.2011.11.010.

Zhang, F., Cui, Y., Zeng, L., Robinet, J.C., Conil, N. and Talandier, J. (2018a), "Effect of degree of saturation on the unconfined compressive strength of natural stiff clays with consideration of air entry value", *Eng. Geol.*, **237**, 140-148. https://doi.org/10.1016/j.enggeo.2018.02.013.

Zhang, F., Cui, Y.J. and Ye, W.M. (2018b), "Distinguishing macro- and micro-pores for materials with different pore populations", *Geotech. Lett.*, **8**(2), 102-110. https://doi.org/10.1680/jgele.17.00144.

Zhang, J., Niu, G., Li, X. and Sun, D.A. (2020), "Hydro-mechanical behavior of expansive soils with different dry densities over a wide suction range", *Acta Geotech.*, **15**(1), 265-278. https://doi.org/10.1007/s11440-019-00874-y.

Zhang, L. and Chen, Q. (2005), "Predicting bimodal soil-water characteristic curves", *J. Geotech. Geoenviron. Eng.*, **131**(5), 666-670. https://doi.org/10.1061/(ASCE)10900241(2005)131:5(666).

Zhou, A., Sheng, D., Sloan, S.W. and Gens, A. (2012), "Interpretation of unsaturated soil behaviour in the stress-saturation space, I: Volume change and water retention behaviour", *Comput. Geotech.*, **43**, 178-187. https://doi.org/10.1016/j.compgeo.2012.04.010.

Zhou, A., Huang, R. and Sheng, D. (2016), "Capillary water retention curve and shear strength of unsaturated soils", *Can. Geotech. J.*, **53**(6), 974-987. https://doi.org/10.1139/cgj-2015-0322.

Zhou, A., Wu, S., Li, J. and Sheng, D. (2018), "Including degree of capillary saturation into constitutive modelling of unsaturated soils", *Comput. Geotech.*, **95**, 82-98. https://doi.org/10.1016/j.compgeo.2017.09.017.

Zhu, H., Zhang, L., Chen, C. and Chan, K. (2018), "Three-dimensional modelling of water flow due to leakage from pressurized buried pipe", *Geomech. Eng.*, **16**(4), 423-433. https://doi.org/10.12989/gae.2018.16.4.423.

IC